Excision of Uranium Oxide Chains and Ribbons in the Novel One-Dimensional Uranyl Iodates $K_2[(UO_2)_3(IO_3)_4O_2]$ and $Ba[(UO_2)_2(IO_3)_2O_2](H_2O)$

Amanda C. Bean,[†] Michael Ruf,[‡] and Thomas E. Albrecht-Schmitt*[,†]

Department of Chemistry, Auburn University, Auburn, Alabama 36849, and Bruker AXS, 5465 East Cheryl Parkway, Madison, Wisconsin 53711

Received March 28, 2001

The alkali metal and alkaline-earth metal uranyl iodates $K_2[(UO_2)_3(IO_3)_4O_2]$ and $Ba[(UO_2)_2(IO_3)_2O_2](H_2O)$ have been prepared from the hydrothermal reactions of KCl or $BaCl_2$ with UO_3 and I_2O_5 at 425 and 180 °C, respectively. While $K_2[(UO_2)_3(IO_3)_4O_2]$ can be synthesized under both mild and supercritical conditions, the yield increases from <5% to 73% as the temperature is raised from 180 to 425 °C. $Ba[(UO_2)_2(IO_3)_2O_2](H_2O)$, however, has only been isolated from reactions performed in the mild temperature regime. Thermal measurements (DSC) indicate that $K_2[(UO_2)_3(IO_3)_4O_2]$ is more stable than $Ba[(UO_2)_2(IO_3)_2O_2](H_2O)$ and that both compounds decompose through thermal disproportionation at 579 and 575 °C, respectively. The difference in the thermal behavior of these compounds provides a basis for the divergence of their preparation temperatures. The structure of $K_2[(UO_2)_3(IO_3)_4O_2]$ is composed of $^1_\infty[(UO_2)_3(IO_3)_4O_2]^{2-}$ chains built from the edge-sharing UO_7 pentagonal bipyramids and UO_6 octahedra. $Ba[(UO_2)_2(IO_3)_2O_2](H_2O)$ consists of one-dimensional $^1_\infty[(UO_2)_2(IO_3)_2O_2]^{2-}$ ribbons formed from the edge sharing of distorted UO_7 pentagonal bipyramids. In both compounds the iodate groups occur in both bridging and monodentate binding modes and further serve to terminate the edges of the uranium oxide chains. The K^+ or Ba^{2+} cations separate the chains or ribbons in these compounds forming bonds with terminal oxygen atoms from the iodate ligands. Crystallographic data: $K_2[(UO_2)_3(IO_3)_4O_2]$, triclinic, space group $P\bar{1}$, $a = 7.0372(5)$ Å, $b = 7.7727(5)$ Å, $c = 8.9851(6)$ Å, $\alpha = 93.386(1)°$, $\beta = 105.668(1)°$, $\gamma = 91.339(1)°$, $Z = 1$; $Ba[(UO_2)_2(IO_3)_2O_2](H_2O)$, monoclinic, space group $P2_1/c$, $a = 8.062(4)$ Å, $b = 6.940(3)$ Å, $c = 21.67(1)$, $\beta = 98.05(1)°$, $Z = 4$.

Introduction

Contemporary studies on uranium compounds have focused primarily on the preparation of inorganic/organic hybrids under mild hydrothermal conditions. These investigations have afforded a large series of low-dimensional and open-framework fluorides and oxyfluorides,[1−10] phosphates,[11] and molybdates.[12] While the chemistry of uranium under hydrothermal conditions is greatly influenced by choice of template, reaction temperature, and pH, the range of chemical and physical properties of these compounds can be significantly expanded through the use of polydentate ligands with variable binding modes such as tellurites,[13−17] germanates,[18−23] and silicates.[24−26] These and other ligands can further impart chemical, structural, and physical properties not obtainable with redox inactive and structurally inflexible ligands.

Using these aforementioned concepts, we have begun the exploration of uranyl iodates, for which there are very few well-established examples. While uranyl iodates have been reported in the past, the characterization of these compounds has been

[†] Auburn University.
[‡] Bruker AXS.

(1) Almond, P. M.; Talley, C. E.; Bean, A. C.; Peper, S. M.; Albrecht-Schmitt; T. E. *J. Solid State Chem*. **2000**, *154*, 635.
(2) Talley, C. E.; Bean, A. C.; Albrecht-Schmitt, T. E. *Inorg. Chem.* **2000**, *39*, 5174.
(3) Francis, R. J.; Halasyamani, P. S.; O'Hare, D. *Angew. Chem., Int. Ed.* **1998**, *37*, 2214.
(4) Francis, R. J.; Halasyamani, P. S.; O'Hare, D. *Chem. Mater*. **1998**, *10*, 3131.
(5) Allen, S.; Barlow, S.; Halasyamani, P. S.; Mosselmans, J. F. W.; O'Hare, D.; Walker, S. M.; Walton, R. I. *Inorg. Chem.* **2000**, *39*, 3791.
(6) Almond, P. M.; Deakin, L.; Porter, M. J.; Mar, A.; Albrecht-Schmitt, T. E. *Chem. Mater*. **2000**, *12*, 3208.
(7) Almond, P. M.; Deakin, L. Mar, A.; Albrecht-Schmitt, T. E. *Inorg. Chem.* **2001**, *40*, 866.
(8) Halasyamani, P. S.; Walker, S. M.; O'Hare, D. *J. Am. Chem. Soc.* **1999**, *121*, 7415.
(9) Walker, S. M.; Halasyamani, P. S.; Allen, S.; O'Hare, D. *J. Am. Chem. Soc.* **1999**, *121*, 10513.
(10) Francis, R. J.; Halasyamani, P. S.; Bee, J. S.; O'Hare, D. *J. Am. Chem. Soc.* **1999**, *121*, 1609.
(11) Francis, R. J.; Drewitt, M. J.; Halasyamani, P. S.; Ranganathachar, C.; O'Hare, D.; Clegg, W.; Teat, S. J. *Chem. Commun.* **1998**, *2*, 279.
(12) Halasyamani, P. C.; Francis, R. J.; Walker, S. M.; O'Hare, D. *Inorg. Chem.* **1999**, *38*, 271.
(13) Feger, C. R.; Schimek, G. L.; Kolis, J. W. *J. Solid State Chem.* **1999**, *143*, 246.
(14) Feger, C. R.; Kolis, J. W.; Gorny, K.; Pennington, W. T. *J. Solid State Chem.* **1999**, *143*, 254.
(15) Feger, C. R.; Kolis, J. W. *Acta Crystallogr.* **1998**, *C54*, 1217.
(16) Feger, C. R.; Kolis, J. W. *Acta Crystallogr.* **1998**, *C54*, 1055.
(17) Feger, C. R.; Kolis, J. W. *Inorg. Chem.* **1998**, *37*, 4046.
(18) Bu, X. H.; Feng, P. Y.; Stucky, G. D. *Chem. Mater.* **2000**, *12*, 1811.
(19) Bu, X. H.; Feng, P. Y.; Stucky, G. D. *Chem. Mater.* **2000**, *12*, 1505.
(20) Bu, X. H.; Feng, P. Y.; Stucky, G. D. *Chem. Mater.* **1999**, *11*, 3423.
(21) Bu, X. H.; Feng, P. Y.; Geier, T. E. Zhao, D. Y.; Stucky, G. D. *J. Am. Chem. Soc.* **1998**, *120*, 13389.
(22) Li, H. L.; Eddaoudi, M.; Yaghi, O. M. *Angew. Chem., Int. Ed.* **1999**, *38*, 653.
(23) O'Keefe, M.; Yaghi, O. M. *Chem.—Eur. J.* **1999**, *5*, 2796.
(24) Burns, P. C.; Ewing, R. C.; Hawthorne, F. C. *Can. Mineral.* **1997**, *35*, 1551.
(25) Burns, P. C. In *Uranium: Mineralogy, Geochemistry and the Environment*; Burns, P. C., Finch, R., Eds.; Mineralogical Society of America: Washington, DC, 1999; Chapter 1.
(26) Burns, P. C.; Miller, M. L.; Ewing, R. C. *Can. Mineral.* **1996**, *34*, 845.

10.1021/ic010342l CCC: $20.00
Published on Web 06/30/2001

highly limited.[27,28] In the presence of oxidizing iodate ligands, uranium has thus far only been isolated in the hexavalent oxidation state, which generally occurs in the form of a linear uranyl, UO_2^{2+}, unit.[26,29,30] The uranyl cation, however, shows substantial structural diversity as up to six additional ligands can be incorporated into the equatorial plane. This gives rise to six-coordinate $[UO_2X_4]^{n-}$ octahedra, seven-coordinate $[UO_2X_5]^{n-}$ pentagonal bipyramids, and eight-coordinate $[UO_2X_6]^{n-}$ hexagonal bipyramids.[24−26] Some uranium-bearing minerals contain multiple types of uranyl polyhedra giving rise to stunning levels of structural complexity as found in wölsendorfite, $Pb_{6.16}Ba_{0.36}[(UO_2)_{14}O_{19}(OH)_4](H_2O)_{12}$.[31] We have established that the hydrothermal chemistry of even the simple uranyl iodates $UO_2(IO_3)_2$ and $UO_2(IO_3)_2(H_2O)$ is actually highly complex and that the structures of these compounds are unique to this system.[28,32]

Iodates in general have a propensity for crystallizing in noncentrosymmetric space groups, and therefore the possibility exists for preparing uranyl iodates with atypical physical properties.[33−35] Our interest in these compounds, however, is based on the presence of two redox active centers with strong oxidizing abilities and a stereochemically active lone pair, making these compounds applicable to the development of selective oxidation catalysts.[36−38] Furthermore, the stabilities of uranyl iodates may play an important role in the fate of ^{129}I in nuclear fuel waste.[39] Therefore, the chemistry of uranyl iodates is of importance as it relates to the long-term storage of nuclear reactor waste, especially if seepage into groundwater occurs.[24,39−42] Herein we report the hydrothermal syntheses, structural characterization, vibrational spectroscopy, and thermal behavior of two one-dimensional uranyl iodates with unprecedented structures, $K_2[(UO_2)_3(IO_3)_4O_2]$ and $Ba[(UO_2)_2(IO_3)_2O_2](H_2O)$. These compounds are further illustrations of the striking differences between mild and supercritical hydrothermal reaction conditions.[43,44]

Experimental Section

Syntheses. UO_3 (99.8%, Alfa-Aesar), I_2O_5 (98%, Alfa-Aesar), KCl (Ultrapure, Alfa-Aesar), and $BaCl_2$ (99.999%, Alfa-Aesar) were used as received. Distilled and Millipore filtered water was used in all reactions. The resistance of the water was 18.2 MΩ. Quartz tubes were rinsed with distilled and Millipore filtered water and dried in an oven prior to use. ***CAUTION:*** *While the UO_3 contains depleted U, standard precautions for handling radioactive materials should be followed. Extreme care should always be taken when scoring and opening sealed tubes from hydrothermal reactions since these are typically under pressure. These tubes should always be frozen in liquid nitrogen and scored while wearing thick gloves and a full-face shield.* SEM/EDX analyses were performed using a JEOL 840/Link Isis instrument. Ba, I, and K percentages were calibrated against standards. Typical results are within 3% of actual ratios. IR spectra were collected on a Nicolet 5PC FT-IR spectrometer from KBr pellets.

$K_2[(UO_2)_3(IO_3)_4O_2]$. UO_3 (62 mg, 0.22 mmol), I_2O_5 (72 mg, 0.22 mmol), and KCl (16 mg, 0.22 mmol) were loaded in a quartz tube and mixed by shaking the tube. Water (0.6 mL) was then added to the solids, which represents a fill level of approximately 45%. The tube was then frozen in liquid nitrogen, evacuated, and sealed. The tube was then placed in a Leco Tem-Press 27-mL autoclave, and the remainder of the volume of the autoclave was filled with water. The autoclave was sealed, placed in a vertical tube furnace, and heated at 10 °C/min to 425 °C. After 72 h the furnace was cooled over 24 h to 23 °C. The tube was subsequently removed from the autoclave and frozen in liquid nitrogen to allow for safe opening. The solid product consisted of golden needles of $K_2[(UO_2)_3(IO_3)_4O_2]$ and elemental iodine. The solids were washed with methanol (removing iodine) and allowed to dry; yield, 85 mg (73% yield based on U). EDX analysis for $K_2[(UO_2)_3(IO_3)_4O_2]$ provided a K:U:I ratio of 2:3:4. IR (KBr, cm^{-1}): ν(U═O) 896 (s); ν(U═O, U−O, and I═O) 862 (s), 829 (s), 794 (s), 787 (s), 742 (s), 719 (s), 691 (s, b), 501 (s, b), 443 (m).

$Ba[(UO_2)_2(IO_3)_2O_2](H_2O)$. UO_3 (286 mg, 1 mmol), I_2O_5 (334 mg, 1 mmol), and $BaCl_2$ (244 mg, 1 mmol) were loaded in a 23-mL PTFE-lined autoclave. Water (1.5 mL) was then added to the solids. The autoclave was sealed, placed in a box furnace, and heated to 180 °C. After 72 h the furnace was cooled at 9 °C/h to 23 °C. The product consisted of a pale yellow solution over golden needles of $Ba[(UO_2)_2(IO_3)_2O_2](H_2O)$, yellow truncated tetragonal bipyramids of $UO_2(IO_3)_2(H_2O)$, and iodine. The mother liquor was decanted from the crystals, which were then washed with water and methanol (removing iodine) and allowed to dry; yield, 323 mg (60% yield based on U). EDX analysis for $Ba[(UO_2)_2(IO_3)_2O_2](H_2O)$ provided a Ba:U:I ratio of 1:2:2. IR (KBr, cm^{-1}): ν(U═O) 904 (s, sh); ν(U═O, U−O, and I═O) 862 (s), 831 (s), 790 (s), 775 (s), 713 (s), 570, (m, sh) 524 (m), 455 (s).

Crystallographic Studies. Golden crystals of $K_2[(UO_2)_3(IO_3)_4O_2]$ and $Ba[(UO_2)_2(IO_3)_2O_2](H_2O)$ with the dimensions of 0.65 mm × 0.03 mm × 0.03 mm and 0.235 mm × 0.023 mm × 0.018 mm, respectively, were mounted on glass fibers and aligned on a Bruker SMART APEX CCD X-ray diffractometer. Intensity measurements were performed using graphite-monochromated Mo Kα radiation from a sealed tube and a monocapillary. SMART was used for preliminary determination of the cell constants and data collection control. For $K_2[(UO_2)_3(IO_3)_4O_2]$, the intensities of reflections of a sphere were collected by a combination of 6 sets of exposures (frames). Each set had a different ϕ angle for the crystal, and each exposure covered a range of 0.3° in ω. A total of 3600 frames were collected with an exposure time per frame of 6 s.

Crystals of $Ba[(UO_2)_2(IO_3)_2O_2](H_2O)$ proved to be twins, and RLATT was used to separate reflections from different domains of the twinned sample for indexing with SMART. GEMINI determined the twin law as a 2° rotation around reciprocal [010]. The intensities of reflections of a sphere were collected by a combination of 3 sets of exposures (frames). Each set had a different ϕ angle for the crystal, and each exposure covered a range of 0.3° in ω. A total of 1800 frames were collected with an exposure time per frame of 30 s.

For both $K_2[(UO_2)_3(IO_3)_4O_2]$ and $Ba[(UO_2)_2(IO_3)_2O_2](H_2O)$, determination of integral intensities and global cell refinement were performed with the Bruker SAINT (v 6.02) software package using a

(27) (a) Tsivadze, A. Y.; Krot, N. N.; Muchnik, B. I. *Proc. Moscow Symp. Chem. Transuranium Elem.* 1976, 89−94. (b) Tsivadze, A. Y.; Muchnik, B. I. Krot, N. N. *Zh. Neorg. Khim.* **1972**, *17*, 3324.
(28) Weigel, F.; Engelhardt, L. W. H. *J. Less-Common Met.* **1983**, *91*, 339.
(29) Carnall, W. T.; Crosswhite, H. M. In *The Chemistry of the Actinide Elements*; Katz, J. J., Seaborg, G. T., Morss, J. R., Eds.; Chapman and Hall: London, 1986.
(30) Kraus, K. A.; Nelson, F.; Johnson, G. L. *J. Am. Chem. Soc.* **1949**, *71*, 2510.
(31) Burns, P. C. *Am. Mineral.* **1999**, *84*, 1661.
(32) Bean, A. C.; Peper, S. M.; Albrecht-Schmitt, T. E. *Chem. Mater.* **2001**, *13*, 1266.
(33) Bergman, J. G.; Boyd, G. D.; Ashkin, A.; Kurtz, S. K. *J. Appl. Phys.* **1969**, *40*, 2860.
(34) Keve, E. T.; Abrahams, S. C.; Bernstein, J. L. *J. Chem. Phys.* **1971**, *54*, 2556.
(35) (a) Nassua, K.; Shiever, J. W.; Prescott, B. E. *J. Solid State Chem.* **1973**, *7*, 186. (b) Abrahams, S. C.; Sherwood, R. C.; Bernstein, J. L.; Nassau, K. *J. Solid State Chem.* **1973**, *7*, 205.
(36) Hutchings, G. J.; Heneghan, C. S.; Hudson, I. D.; Taylor, S. H. *Nature* **1996**, *384*, 341−343.
(37) Collette, H.; Deremince-Mathieu, V.; Gabelica, Z.; Nagy, J. B.; Derouane, E. G.; Verbist, J. J. *J. Chem. Soc., Faraday Trans. 2* **1987**, *83*, 1263.
(38) Gates, B. C. *Catalytic Chemistry*; Wiley: New York, 1992; Chapter 6.
(39) Burns, P. C. Personal communication.
(40) Clark, D. L.; Hobart, D. E.; Neu, M. P. *Chem. Rev.* **1995**, *95*, 25.
(41) Clark, D. L.; Conradson, S. D.; Ekberg, S. A.; Hess, N. J.; Neu, M. P.; Palmer, P. D.; Runde, W.; Tait, C. D. *J. Am. Chem. Soc.* **1996**, *118*, 2089.
(42) Kaszuba, J. P.; Runde, W. H. *Environ. Sci. Technol.* **1999**, *33*, 4427.
(43) Korzenski, M. B.; Kolis, J. W.; Long, G. L. *J. Solid State Chem.* **1999**, *147*, 390.
(44) Kolis, J. W.; Korzenski, M. B. In *Chemical Synthesis Using Supercritical Fluids*; Jessop, P. G., Leitner, W., Eds.; Wiley-VCH: New York, 1999; pp 213−241.

Table 1. Crystallographic Data for $K_2[(UO_2)_3(IO_3)_4O_2]$ and $Ba[(UO_2)_2(IO_3)_2O_2](H_2O)$

formula	$K_2[(UO_2)_3(IO_3)_4O_2]$	$Ba[(UO_2)_2(IO_3)_2O_2](H_2O)$
formula mass (amu)	1619.89	1077.22
space group	$P\bar{1}$ (No. 2)	$P2_1/c$ (No. 14)
a (Å)	7.0372(5)	8.062(4)
b (Å)	7.7727(5)	6.940(3)
c (Å)	8.9851(6)	21.67(1)
α (deg)	93.386(1)	90
β (deg)	105.668(1)	98.05(1)
γ (deg)	91.339(1)	90
V (Å$^{3)}$	471.98(6)	1200.2(9)
Z	1	4
T (°C)	−100	25
λ (Å)	0.710 73	0.710 73
ρ_{calcd} (g cm^{-3})	5.699	5.950
μ(Mo Kα) (cm^{-1})	327.49	353.70
$R(F)$ for $F_o^2 > 2\sigma(F_o^2)^a$	0.0303	0.0591
$R_w(F_o^2)^b$	0.0751	0.1118

^{a} $R(F) = \sum||F_o| - |F_c||/\sum|F_o|$. ^{b} $R_w(F_o^2) = [\sum[w(F_o^2 - F_c^2)^2]/\sum wF_o^4]^{1/2}$.

narrow-frame integration algorithm. A semiempirical absorption correction was applied based on the intensities of symmetry-related reflections measured at different angular settings using SADABS.[45] The program suite SHELXTL (v 5.1) was used for space group determination (XPREP), structure solution (XS), and refinement (XL).[46] Uranium, barium, and iodine atoms dominate the X-ray scattering in $Ba[(UO_2)_2(IO_3)_2O_2](H_2O)$, making the determination of hydrogen positions for the water molecule unreliable, and they were not included in the structural model. The final refinement included displacement parameters for all atoms and a secondary extinction parameter. Some crystallographic details are listed in Table 1 for $K_2[(UO_2)_3(IO_3)_4O_2]$ and $Ba[(UO_2)_2(IO_3)_2O_2](H_2O)$; additional details can be found in the Supporting Information.

Differential Scanning Calorimetry Measurements. Thermal data for $K_2[(UO_2)_3(IO_3)_4O_2]$ and $Ba[(UO_2)_2(IO_3)_2O_2](H_2O)$ were collected using a TA Instruments model 2920 differential scanning calorimeter (DSC). Samples (20 mg) were encapsulated in aluminum pans and heated at 10 °C/min from 25 to 600 °C under a nitrogen atmosphere.

Results and Discussion

Syntheses. The reaction of UO_3 with I_2O_5 in the presence of KCl in aqueous media at 425 °C for 72 h results in the formation of $K_2[(UO_2)_3(IO_3)_4O_2]$ in 73% yield, reaction 1. While $K_2[(UO_2)_3(IO_3)_4O_2]$ can be prepared under both mild and supercritical conditions, the yield increases from <5% to 73% as the temperature is raised from 180 to 425 °C. Furthermore, the crystal size improves from microcrystals of poor quality to high-quality single crystals as long as 3 mm. In addition, we have explored varying starting material ratios and inevitably found that $K_2[(UO_2)_3(IO_3)_4O_2]$ is the only potassium-containing product formed. Reactions with decreased potassium content also produce $UO_2(IO_3)_2$ and $UO_2(IO_3)_2(H_2O)$.[32] At low temperatures, $UO_2(IO_3)_2(H_2O)$ becomes the dominant product of these reactions.

$$2KCl + 3UO_3 + 2I_2O_5 + H_2O \xrightarrow[H_2O]{425\ ^\circ C,\ 3\ days} K_2(UO_2)_3(IO_3)_4O_2 + 2HCl \quad (1)$$

In contrast to the need for supercritical conditions in the synthesis of $K_2[(UO_2)_3(IO_3)_4O_2]$ in reasonable yield, the reaction of $BaCl_2$ with UO_3 and I_2O_5 produces $Ba[(UO_2)_2(IO_3)_2O_2](H_2O)$ in 60% yield only under relatively mild hydrothermal conditions, reaction 2. $UO_2(IO_3)_2(H_2O)$ is also isolated from this reaction. $Ba[(UO_2)_2(IO_3)_2O_2](H_2O)$ can also be prepared in quartz tubes with a reaction temperature of 180 °C. In the syntheses of both $K_2[(UO_2)_3(IO_3)_4O_2]$ and $Ba[(UO_2)_2(IO_3)_2O_2](H_2O)$ small amounts of I_2 are produced, most likely through thermal disproportionation of IO_3^-. Washing the product mixtures with methanol rapidly removes I_2 so that it does not interfere in subsequent characterization. In the absence of water, solid-state reactions involving UO_3 and I_2O_5 produce ill-defined product mixtures in the form of powders with the majority of the I_2O_5 having undergone thermal decomposition or disproportionation.

$$BaCl_2 + 2UO_3 + I_2O_5 + 2H_2O \xrightarrow[H_2O]{180\ ^\circ C,\ 3\ days} Ba[(UO_2)_2(IO_3)_2O_2](H_2O) + 2HCl \quad (2)$$

The choice of utilizing chloride salts as sources of alkali and alkaline-earth metal cations is based on our observations that, in hydrothermal reactions of U(VI), chloride is easily exchanged with harder ligands such as oxo donors and fluoride. Furthermore, the chloride anions can serve as mineralizing agents aiding both in the dissolution of UO_3 and in the formation of single crystals. EDX measurements establish that chloride is not incorporated into these compounds.

Thermal Behavior. The thermal behavior of uranium-bearing minerals and compounds has been reviewed extensively by Čejka.[47] Differential scanning calorimetry (DSC) and thermogravimetric analysis (TGA) measurements have been reported for $UO_2(IO_3)_2$ and $UO_2(IO_3)_2(H_2O)$ by our group.[32] DSC measurements indicate that $K_2[(UO_2)_3(IO_3)_4O_2]$ undergoes a small endothermic transformation at 491 °C and decomposes at 579 °C. Decomposition probably occurs through thermal disproportionation of iodate as we have noted similar thermal disproportionation temperatures for $UO_2(IO_3)_2$ and $UO_2(IO_3)_2(H_2O)$.[32] Unfortunately, we have been unable to isolate new products from hydrothermal reactions of KCl with UO_3 and I_2O_5 above 500 °C. $Ba[(UO_2)_2(IO_3)_2O_2](H_2O)$ shows lower thermal stability with respect to $K_2[(UO_2)_3(IO_3)_4O_2]$ not only through the expected loss of water at low temperatures (210 °C) but also through a series of low-temperature, small endotherms at 304, 358, 420, and 491 °C prior to a large endotherm at 553 °C and thermal disproportionation at 575 °C. While the details of the thermal transformations of these compounds prior to decomposition are not understood, these substantial differences probably account for the variations in the preparation temperatures of these compounds and indicate the importance of exploring hydrothermal syntheses in multiple temperature regimes. Thermograms for $K_2[(UO_2)_3(IO_3)_4O_2]$ and $Ba[(UO_2)_2(IO_3)_2O_2](H_2O)$ are given in the Supporting Information.

Structures. $K_2[(UO_2)_3(IO_3)_4O_2]$. The structure of $K_2[(UO_2)_3(IO_3)_4O_2]$ consists of infinite one-dimensional $^1_\infty[(UO_2)_3(IO_3)_4O_2]^{2-}$ chains running down the a-axis. These chains are constructed from dimers of edge-sharing UO_7 pentagonal bipyramids that are linked together with distorted UO_6 octahedra. This creates a zigzagging uranium oxide chain as depicted in Figure 1a. A polyhedral representation of this structure is shown in Figure 1b. This is the first observation of this type of

(45) *SADABS*. Program for absorption correction using SMART CCD based on the method of Blessing: Blessing, R. H. *Acta Crystallogr.* **1995**, *A51*, 33−38.

(46) Sheldrick, G. M. *SHELXTL PC, Version 5.0, An Integrated System for Solving, Refining, and Displaying Crystal Structures from Diffraction Data*; Siemens Analytical X-Ray Instruments, Inc.: Madison, WI, 1994.

(47) Čejka, J. In *Uranium: Mineralogy, Geochemistry and the Environment*; Burns, P. C., Finch, R., Eds.; Mineralogical Society of America: Washington, DC, 1999; Chapter 1.

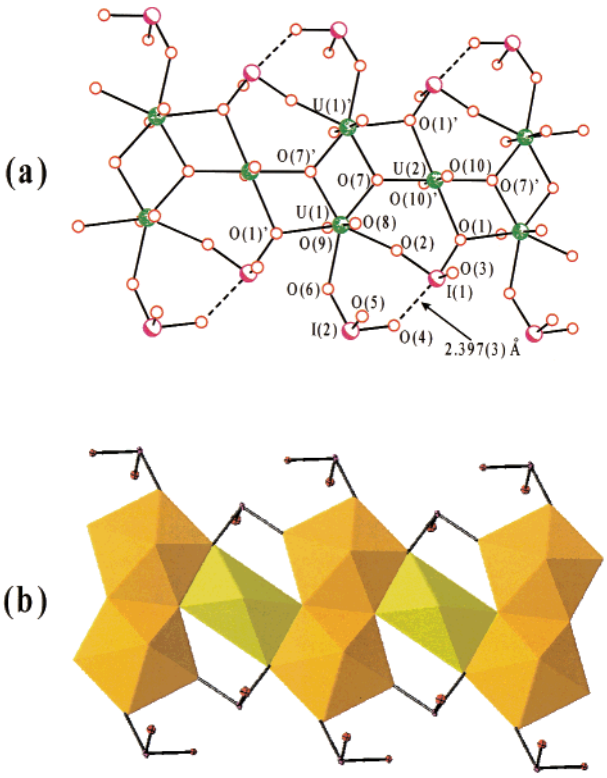

Figure 1. (a) Infinite one-dimensional $^{1}_{\infty}[(UO_2)_3(IO_3)_4O_2]^{2-}$ chains constructed from dimers of edge-sharing UO_7 pentagonal bipyramids that are linked together with distorted UO_6 octahedra running down the *a*-axis in $K_2[(UO_2)_3(IO_3)_4O_2]$. (b) A polyhedral representation of the one-dimensional chains in $K_2[(UO_2)_3(IO_3)_4O_2]$ with UO_7 pentagonal bipyramids shown in orange and UO_6 octahedra in yellow.

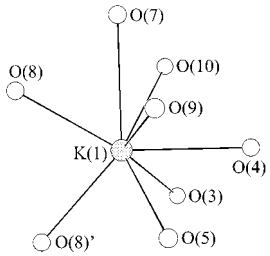

Figure 2. Bicapped trigonal prismatic coordination geometry of the K^+ cations in $K_2[(UO_2)_3(IO_3)_4O_2]$.

connectivity in one-dimensional uranyl-containing structures.[25,26] The K^+ cations separate the chains from one another and are coordinated by terminal oxygen atoms from iodate ligands. The iodate ligands adopt both bridging and monodentate binding modes. The bridging iodates link the dimers of edge-sharing UO_7 pentagonal bipyramids and form two opposite corners of the distorted UO_6 octahedra. The monodentate iodates are solely bound to the UO_7 polyhedra. Both types of iodates terminate the edges of these one-dimensional chains. The remaining oxide ligands are μ_3-O atoms and are corners mutually shared by the dimers of edge-sharing UO_7 pentagonal bipyramids and the UO_6 octahedra. The K^+ cations are coordinated by eight oxygen atoms from the iodate ligands in a bicapped trigonal prismatic geometry as illustrated in Figure 2. The capping of the prism occurs on one rectangular face and on one of the ends of the trigonal prism. However, the latter capping atom lies 3.149(4) Å away from the potassium center, which is approximately 0.2 Å farther than the other oxygen atoms.

The U−O bond lengths for the UO_7 units range from 1.796(4) Å for U═O bonds of the uranyl unit to 2.251(3)−2.409(3) Å for U−O bonds in the equatorial plane. U−O bond lengths for the distorted UO_6 octahedra vary from 1.791(4) Å for U═O bonds of the uranyl unit to 2.217(3)−2.451(3) Å for U−O bonds in the equatorial plane. The longest U−O bonds for both types of polyhedra are created with the μ_3-O atom of the bridging iodate. Iodate ligands in $UO_2(IO_3)_2$ also contain oxygen atoms that adopt μ_3 binding modes.[32] However, the iodate groups in $UO_2(IO_3)_2$ chelate the uranium centers. As O(1) is the μ_3 atom, the I═O bond distance of 1.856(3) Å is lengthened with respect to the other two I═O bond distances of 1.778(4) and 1.805(3) Å. I═O bond lengths for the monodentate iodate are 1.791(3), 1.808(3), and 1.818(3) Å and show far less variation than the bridging iodate group. In addition, there are close I···O contacts of 2.397(3) Å between the terminal oxygen atoms from the monodentate iodate ligand and the neighboring iodine atom from the iodate that bridges uranium centers. These types of contacts are common in iodate structures and have also been observed in both $UO_2(IO_3)_2$ and $UO_2(IO_3)_2(H_2O)$.[32] An important difference between $K_2(UO_2)_3(IO_3)_4O_2$ and the two aforementioned compounds is that interchain and interlayer I···O interactions have been replaced by K−O(IO_3^-) ionic bonds. K−O bond distances range from 2.694(4) to 3.149(4) Å. Selected bond lengths are given in Table 2. Bond valence sum calculations provide values of 6.140 and 5.841 for U(1) and U(2), respectively.[48,49] Parameters for seven- and six-coordinate U(VI) from Burns et al. were used in this calculation.[24]

Table 2. Selected Bond Distances (Å) for $K_2[(UO_2)_3(IO_3)_4O_2]$

U(1)−O(1)	2.409(3)	I(2)−O(4)	1.808(3)
U(1)−O(2)	2.359(3)	I(2)−O(5)	1.791(3)
U(1)−O(6)	2.398(3)	I(2)−O(6)	1.818(3)
U(1)−O(7)	2.251(3)	I(1)···O(4)	2.397(3)
U(1)−O(7)′	2.262(3)	K(1)−O(3)	2.694(4)
U(1)−O(8) (U═O)	1.796(4)	K(1)−O(4)	2.957(3)
U(1)−O(9) (U═O)	1.796(4)	K(1)−O(5)	2.701(3)
U(2)−O(1)	2.451(3) (×2)	K(1)−O(7)	3.149(4)
U(2)−O(7)	2.217(3) (×2)	K(1)−O(8)	2.789(4)
U(2)−O(10) (U═O)	1.791(4) (×2)	K(1)−O(8)′	2.811(4)
I(1)−O(1)	1.856(3)	K(1)−O(9)	2.783(4)
I(1)−O(2)	1.805(3)	K(1)−O(10)	2.785(4)
I(1)−O(3)	1.778(4)		

Ba[$(UO_2)_2(IO_3)_2O_2$](H_2O**).** The structure of Ba[$(UO_2)_2(IO_3)_2O_2$](H_2O) consists of edge-sharing distorted pentagonal bipyramidal UO_7 units that form one-dimensional uranium oxide ribbons whose edges are terminated by iodate ligands as shown in Figure 3a. These ribbons run down the *b*-axis and are separated by the Ba^{2+} cations and water molecules. This compound also displays a new structural motif for one-dimensional hexavalent uranium compounds. As in $K_2[(UO_2)_3(IO_3)_4O_2]$, there are two crystallographically unique uranium centers. However, in this structure both uranium atoms are seven-coordinate, highly distorted pentagonal bipyramids. The pentagonal bipyramids containing U(1) share two edges with neighboring polyhedra, and these units line the edges of the ribbons, whereas the pentagonal bipyramids containing U(2) are on the interior of the ribbons and share four edges with neighboring polyhedra as shown in Figure 3b. The iodate ligands adopt both monodentate and bridging binding modes and terminate the edges of the ribbon as found in $K_2[(UO_2)_3(IO_3)_4O_2]$. The Ba^{2+} cations are contained within distorted tricapped trigonal prisms where two rectangular faces and one triangular face are capped (Figure 4). Again, the longest distance is to the oxygen atom capping the triangular face (3.145(11) Å).

The U═O bond lengths of 1.793(11) and 1.821(9) Å for U(1) and 1.823(10) and 1.835(10) Å for U(2) are within expected

(48) Brown, I. D.; Altermatt, D. *Acta Crystallogr.* **1985**, *B41*, 244.
(49) Brese, N. E.; O'Keeffe, M. *Acta Crystallogr.* **1991**, *B47*, 192.

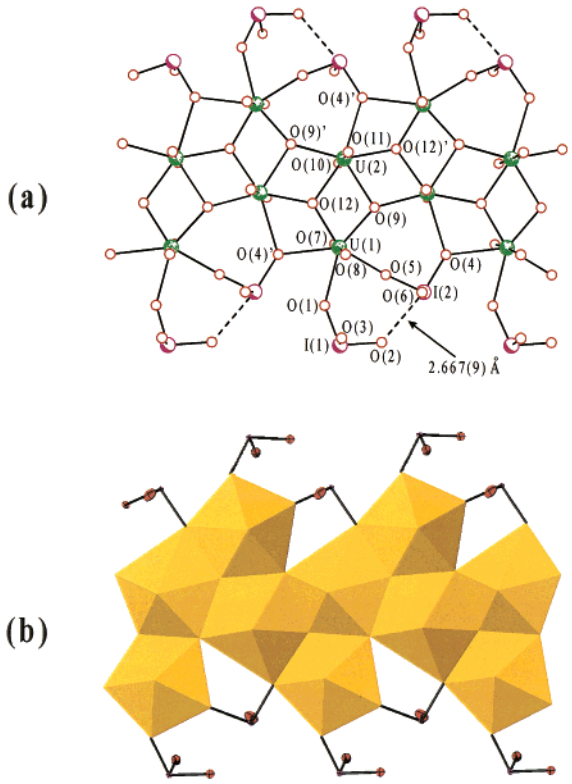

Figure 3. (a) One-dimensional $^{1}_{\infty}[(UO_2)_2(IO_3)_2O_2]^{2-}$ ribbons in the structure of $Ba[(UO_2)_2(IO_3)_2O_2](H_2O)$ consisting of edge-sharing distorted pentagonal bipyramidal UO_7 units. (b) A polyhedral representation of the one-dimensional ribbons built from edge-sharing distorted pentagonal bipyramids in $Ba[(UO_2)_2(IO_3)_2O_2](H_2O)$.

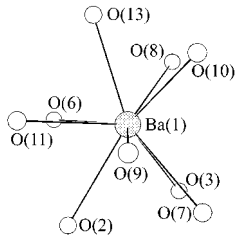

Figure 4. Ba^{2+} cations in $Ba[(UO_2)_2(IO_3)_2O_2](H_2O)$ in a distorted tricapped trigonal prismatic environment where two rectangular faces and one triangular face are capped.

ranges for uranyl moieties. The equatorial bond lengths, which range from 2.153(8) to 2.533(9) Å for U(1) and 2.252(8) to 2.663(9) Å for U(2), show substantial variation in bond distances beyond what is normally observed. The basis for this distortion is again found with the μ_3-O atom from an iodate ligand with the longest U−O bonds of 2.533(9) and 2.663(9) Å being with this oxygen atom. The shortened U−O bonds are found with the μ_3-oxo ligand within the ribbons. The I═O bond distances range from 1.768(10) to 1.810(10) Å. As in $K_2[(UO_2)_3(IO_3)_4O_2]$, there are I···O contacts; however, these are approximately 0.3 Å longer than those in $K_2[(UO_2)_3(IO_3)_4O_2]$ with a distance of 2.667(9) Å between the terminal oxygen atoms from the monodentate iodate ligand and the neighboring iodine atom from the iodate that bridges uranium centers. Ba−O contacts occur from 2.66(2) to 3.145(11) Å, with the shortest bond occurring with the bound water molecule. Bond valence sum calculations provide values of 6.127 and 5.813 for U(1) and U(2), respectively.[48,49] Parameters for seven-coordinate U(VI) from Burns et al. were used in this calculation.[24] Selected bond lengths are given in Table 3 for $Ba[(UO_2)_2(IO_3)_2O_2](H_2O)$.

Table 3. Selected Bond Distances (Å) for $Ba[(UO_2)_2(IO_3)_2O_2](H_2O)$

U(1)−O(1)	2.461(9)	I(1)−O(2)	1.775(9)
U(1)−O(4)	2.533(9)	I(1)−O(3)	1.798(10)
U(1)−O(5)	2.309(10)	I(2)−O(4)	1.810(10)
U(1)−O(7) (U═O)	1.821(9)	I(2)−O(5)	1.797(10)
U(1)−O(8) (U═O)	1.793(11)	I(2)−O(6)	1.768(10)
U(1)−O(9)	2.225(9)	Ba(1)−O(2)	2.794(10)
U(1)−O(12)	2.153(9)	Ba(1)−O(3)	2.739(10)
U(2)−O(4)	2.663(9)	Ba(1)−O(6)	2.735(10)
U(2)−O(9)	2.389(10)	Ba(1)−O(7)	2.807(9)
U(2)−O(9)′	2.278(9)	Ba(1)−O(8)	2.848(10)
U(2)−O(10)	1.823(10)	Ba(1)−O(9)	3.146(10)
U(2)−O(11)	1.835(10)	Ba(1)−O(10)	2.776(11)
U(2)−O(12)	2.252(8)	Ba(1)−O(11)	2.851(10)
U(2)−O(12)′	2.263(9)	Ba(1)−O(13)	2.66(2)
I(1)−O(1)	1.808(9)		

Conclusions

While the topologies of the one-dimensional uranium oxide chains and ribbons in $K_2[(UO_2)_3(IO_3)_4O_2]$ and $Ba[(UO_2)_2(IO_3)_2O_2](H_2O)$ have not been previously observed in other compounds, both of these structural motifs can be excised from three-dimensional and two-dimensional layered uranium oxide compounds.[24−26] For instance, the structure of $K_2(UO_2)_3O_3$ contain chains of edge-sharing UO_7 pentagonal bipyramids that are linked together by UO_6 octahedra.[50] The one-dimensional zigzagging chains in $K_2[(UO_2)_3(IO_3)_4O_2]$ can be derived from this structure. Likewise, protasite, $Ba[(UO_2)_3O_3(OH)_2](H_2O)_3$, contains sheets built from edge-sharing UO_7 pentagonal bipyramids that can be cleaved to yield the ribbons found in $Ba[(UO_2)_2(IO_3)_2O_2](H_2O)$.[51] In fact, the mineral billietite, $Ba[(UO_2)_3O_2(OH)_3]_2(H_2O)_4$, possesses both of these sheet topologies.[51]

The trigonal pyramidal, iodate anions in $K_2[(UO_2)_3(IO_3)_4O_2]$ and $Ba[(UO_2)_2(IO_3)_2O_2](H_2O)$ play a unique role in this structural chemistry in that they appear to terminate the edges of the one-dimensional architectures. By comparison, when tetrahedral anions such as sulfate are employed, these units stitch one-dimensional chains and ribbons together to produce two-dimensional sheets as found in zippeite, $K[(UO_2)_2(SO_4)(OH)_3](H_2O)$, which contains ribbons of UO_7 pentagonal bipyramids linked to one another on both edges by sulfate to produce two-dimensional sheets.[52] Iodate and other trigonal pyramidal anions such as selenite and tellurite can, however, bridge between uranyl units to yield layers as found in $UO_2(IO_3)_2(H_2O)$,[32] $Ba[(UO_2)_3(SeO_3)_2O_2](H_2O)_3$,[53] and $UO_2(TeO_3)$.[54] It will be of interest to discover whether iodate continues to terminate chain edges in other alkali metal, alkaline-earth metal, and transition metal uranyl iodates, which is a topic of current efforts in our group.

Acknowledgment. This work was supported by NASA (Alabama Space Grant Consortium) and Auburn University.

Supporting Information Available: DSC thermograms and Figures S1 and S2 depicting portions of the $K_2[(UO_2)_3(IO_3)_4O_2]$ and $Ba[(UO_2)_2(IO_3)_2O_2](H_2O)$ structures. X-ray crystallographic files for $K_2[(UO_2)_3(IO_3)_4O_2]$ and $Ba[(UO_2)_2(IO_3)_2O_2](H_2O)$ in CIF format. This material is available free of charge via the Internet at http://pubs.acs.org.

IC010342L

(50) Saine, M. C. *J. Less-Common Met.* **1989**, *154*, 361.
(51) Pagoaga, M. K.; Appleman, D. E.; Stewart, J. M. *Am. Mineral.* **1987**, *72*, 1230.
(52) Vochten, R.; Van Haverbeke, L.; Van Springel, K.; Blaton, N.; Peeters, O. M. *Can. Mineral.* **1995**, *33*, 1091.
(53) Cooper, M. A.; Hawthorne, F. C. *Can. Mineral.* **1995**, *33*, 1103.
(54) Meunier, G.; Galy, J. *Acta Crystallogr.* **1973**, *B29*, 1251.